Hindawi Publishing Corporation
Journal of Engineering
Volume 2016, Article ID 7615385, 19 pages
http://dx.doi.org/10.1155/2016/7615385

Research Article

The Hysteresis Performance and Restoring Force Model for Corroded Reinforced Concrete Frame Columns

Guifeng Zhao,[1] Meng Zhang,[1] Yaoliang Li,[1] and Dawang Li[2]

[1]*School of Civil Engineering, Zhengzhou University, Zhengzhou 450001, China*
[2]*Guangdong Provincial Key Laboratory of Durability for Marine Civil Engineering, Shenzhen University, Shenzhen 518060, China*

Correspondence should be addressed to Dawang Li; lidw@szu.edu.cn

Received 14 August 2016; Accepted 5 October 2016

Academic Editor: Song Han

A numerical simulation of the hysteresis performance of corroded reinforced concrete (RC) frame columns was conducted. Moreover, the results obtained were compared with experimental data. On this basis, a degenerated three-linearity (D-TRI) restoring force model was established which could reflect the hysteresis performance of corroded RC frame columns through theoretical analysis and data fitting. Results indicated that the hysteretic bearing capacity of frame columns decreased significantly due to corrosion of the rebar. In view of the characteristics of the hysteresis curve, the plumpness of the hysteresis loop for frame columns decreased and shrinkage increased with increasing rebar corrosion. All these illustrated that the seismic energy dissipation performance of frame columns reduced but their brittleness increased. As for the features of the skeleton curve, the trends for corroded and noncorroded members were basically consistent and roughly corresponded to the features of a trilinear equivalent model. Thereby, the existing Clough hysteresis rule can be used to establish the restoring force model applicable to corroded RC frame columns based on that of the noncorroded RC members. The calculated skeleton curve and hysteresis curve of corroded RC frame columns using the D-TRI model are closer to the experimental results.

1. Introduction

The RC frame column is currently one of the most widely used structural forms. With the increase in its service life and the direct or indirect effects of external corrosion media, structural materials will degrade and undergo surface cracking, carbonisation, desquamation, corrosion-induced expansion of the rebar, and so forth, as shown in Figure 1. Of these, rebar corrosion is regarded as the prime factor affecting the changes in the durability of concrete structures [1, 2]. Corrosion leads to the degradation of geometric parameters and mechanical properties of rebar and, to some extent, will weaken the static bearing capacity of a structure and increase its brittleness. Meanwhile, the seismic performance will be inevitably impaired [3–5].

A frame column, which supports structures such as beams and slabs, is considered the foremost load-bearing member in an RC framed structure. Once a frame column is broken, it exerts a more severe influence on the damage suffered by beams, slabs, and filler walls. As for the frame structures constructed in areas where earthquake frequently occurs, the frame column bears not only the vertical load, but also the brunt of any seismic action. The frame column, as a kind of eccentric compression member, has a lower stiffness than that of the beam and bears mainly vertical load. Therefore, even if only a small number of columns are damaged in a frame structure, the whole structure is likely to collapse (Figure 2). Considering the aforementioned reasons, engineers in different countries try to improve the bearing capacity, ductility, and resistance to lateral displacement, of frame columns as much as possible, so as to endow the frame structure with reliable seismic behaviour.

The hysteresis curve and restoring force model are two important indicators used when analysing the seismic behaviour of RC frame columns [8, 9]. When giving the expectation of ground motion in a mathematical model or inputting certain seismic waves for the region where a structure is located, a restoring force model and its parameters are the most important factors influencing the results of the seismic response analysis of the structure. The hysteresis

(a) Beam (b) Column

Figure 1: Cracks, desquamation of concrete cover, and corrosion of rebar in the frame beam and column.

Figure 2: Earthquake damage to the bottom columns in a frame structure.

performance and restoring force model are mainly influenced by factors such as the size of the members, reinforcement ratio, loading system, and material properties [10–12].

The hysteresis curve reflects the characteristics of structures or members during repetitive stress, including deformation, stiffness degradation, and energy consumption [14–16]. The restoring force model of members refers to the capacity of members to restore themselves to their original column form after unloading and shows the mathematical relationship between restoring force and deformation under cyclic loading [14]. Broadly speaking, the restoring force model consists of a skeleton curve and a hysteresis rule. The former draws boundaries for all the hysteresis feature points while the latter reflects the highly nonlinear characteristic of the structure. The restoring force model also represents the seismic behaviour of structures or members in the analysis of the elastoplastic seismic response and can be obtained based on the relationship between the restoring force and deformation through repetitive experiments. In actual application, the relationship curve needs to be abstracted and simplified to form a practical mathematical model.

So far, existing research on the seismic behaviour of engineering structures is mainly conducted on those to be built, while ignoring the relationship between the seismic behaviour and service time of the structure. As a matter of fact, with the extension of the service of RC frame structures, the corrosion and degradation accumulate continuously. Under such circumstances, the original seismic design of structures fails to reflect the seismic safety situation of corroded structures which have been used for a certain time. Therefore, the seismic safety and durability of corroded and degraded RC frame structures need to be reevaluated and tested, so as to clarify the current performance of such structures. Based on the evaluated results, different measures can be applied to reinforce the structures according to the importance of, and extent of the damage to, the structures. After reinforcement, structures are expected to resist possible seismic actions and avoid, or reduce, causalities and economic loss throughout their service lives.

At present, the hysteresis performance and restoring force models for noncorroded RC frame structures or members have been explored widely in engineering. However, there are relatively few research reports on degraded RC structures or members (particularly frame columns) affected by corrosion. Existing studies mainly focus on the evaluation of the macroscopic seismic behaviour and reinforcement effect of reinforced corroded columns [17–19]. In addition, the hysteresis performance of corroded frame columns is generally studied on samples of a few experiments [13, 19, 20]. Considering that the corrosion and degradation of RC members take a long time in most natural environments, conducting simulations in natural conditions takes a long time and costs too much. Therefore, accelerated corrosion tests are commonly used in practice. By changing parameters including the concentration, chemical components, temperature, and flow rate of the corrosive media, the corrosion effect is enhanced and therefore accelerates testing. Obviously, this approach provides favourable support to research into the stress-related properties of corroded RC structures. To obtain an accurate hysteresis curve and a restoring force model for a corroded RC frame column with specific design parameters, a large number of samples need to be prepared

while using an accelerated corrosion test, to acquire sufficient experimental data. While performing this kind of experiment, the preparation of samples takes a long time and is expensive, and few parameters can be considered at any time. Due to these limitations, the hysteresis performance and restoring force model of corroded RC members have not been sufficiently investigated. Owing to the absence of simple, feasible, calculation methods for the restoring force model of a corroded RC member, the analysis and evaluation of the seismic safety of large amounts of corroded RC structures in seismic zones cannot be rapidly performed to obtain accurate results. This influences the formulation and implementation of maintenance and reinforcement decisions. Therefore, the investigation of the hysteresis performance and a restoring force model for corroded RC structures or members is deemed important for the analysis and assessment of seismic reliability and the maintenance and reinforcement of structures [3–5, 21].

With the rapid development of nonlinear finite element techniques and computer technology, numerical simulation has been widely applied in civil engineering. Moreover, numerical simulation presents numerous advantages such as short computation time and low cost, and it considers the influences of various parameters. Thereby, numerical simulation is used based on the experimental research to study the hysteresis performance of corroded RC members under different working conditions and obtain sufficient relationship data between the restoring force and deformation. In this way, a simple, practical, mathematical model can be established: this is an easy way to construct the restoring force model of corroded members.

According to the above analysis, an RC frame column was studied in terms of the influences of different corrosion rates on the hysteresis performance of the column using nonlinear FE software ABAQUS. Thereafter, the simulation results were compared with the experimental results to verify the reliability of the FE numerical simulation [13]. On this basis, various corroded members were studied by changing the parameters used in their analysis. Furthermore, by analysing the obtained hysteresis, skeleton, and curves, a restoring force model of corroded RC frame column was constructed. The model was expected to provide a simple, reliable computational basis for seismic safety analysis, reliability assessment, reinforcement, and reconstruction of corroded RC frame structures.

2. Definition of a Constitutive Model for RC Materials in ABAQUS

2.1. Constitutive Model for Concrete. A concrete damaged plasticity (CDP) model is a native constitutive model for concrete materials implicit to the algorithm used in the ABAQUS software. The model was first proposed by Lubliner et al. [22] and improved by Lee and Fenves [23] to apply to nonlinear analysis of concrete structures and members under monotonic and cyclic loading [24, 25]. Owing to the concrete materials being affected by various environmental media in different ways, including weakening effects, such as corrosion and carbonisation by chloride ions and sulphates, and strengthening effects, for example, the action of nitrates, it is difficult to define the effects by any uniform standard [26]. The most common causes of weakening chloride- and sulphate-induced corrosion of concrete were taken as examples in this research [27]. Corrosion only affects the concrete in its protective layer, while it has little influence on the internal core concrete under less serious corrosion. Thereby, the authors suggested determining expressions for the stress-strain relationship of intact concrete cores based on the constitutive relationship recommended by Chinese Standard GB50010-2010, Code for the Design of Concrete Structures [28], and the corroded concrete in the protective layer was only regarded as the bearing capacity reserves of the material, while ignoring its contribution to the strength. The bearing capacity reserve was achieved by setting birth and death elements in ABAQUS.

Table 1: Empirical values of parameters in the CDP model.

Parameter	Ψ	m	α_f	γ	μ
Value	30	0.1	1.16	0.6667	0.0005

Concrete structures, or members, will produce plastic deformation and cracking under low intensity cyclic loading, and both the accumulation of plastic deformation and the expansion of cracks can induce stiffness degradation or softening. So, a damage factor d [29] was used in ABAQUS to describe this stiffness degradation or softening:

$$d = 1 - \frac{\sigma_{\text{true}}/E_0}{\varepsilon^{\text{pl}}\left(1/b_c - 1\right) + \sigma_{\text{true}}/E_0}, \quad \varepsilon^{\text{pl}} = \varepsilon^{\text{in}} \times b_c, \tag{1}$$

where d is the damage factor; σ_{true} is the true stress; E_0 is the initial elastic modulus of the concrete; ε^{in} is the inelastic strain in the concrete; ε^{pl} is the plastic strain in the concrete; b_c is the scale factor between plastic strain and inelastic strain ($0 < b_c < 1$). It was found by trial calculation that the hysteresis behaviour of concrete members could be readily simulated when the pressure b_c was 0.7 and the tension b_c was 0.3 during calculation. In addition, the calculated parameters of the CDP model also cover expansive angle, Ψ; flow potential eccentricity, m; the ratio between the biaxial ultimate compressive strength and the uniaxial ultimate compressive strength α_f; the ratio of secondary stress invariants on the tensile, and compressive meridian planes γ, and bonding parameter μ. After calculation, the suggested values of the above parameters are listed in Table 1.

2.2. Constitutive Model for Rebar

2.2.1. Constitutive Relationship for Noncorroded Rebar. Under cyclic loading, the influence of the Bauschinger effect produced by loading and unloading on the stiffness degradation of rebar must be taken into account. Owing to the actual factors affecting the Bauschinger effect being complicated, some researchers have simplified the constitutive model of rebar based on experimental data to facilitate analysis. Typically, the USTEEL02 subprogram for rebar modelling in the uniaxial hysteresis constitutive model set of PQ-Fibre [7] material developed at Tsinghua University may be used to improve

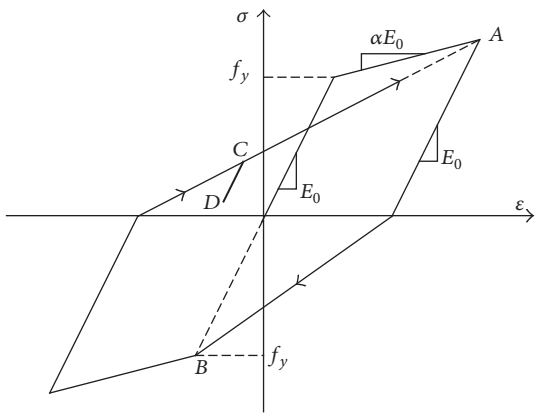

Figure 3: Loading and unloading: the Clough model [6].

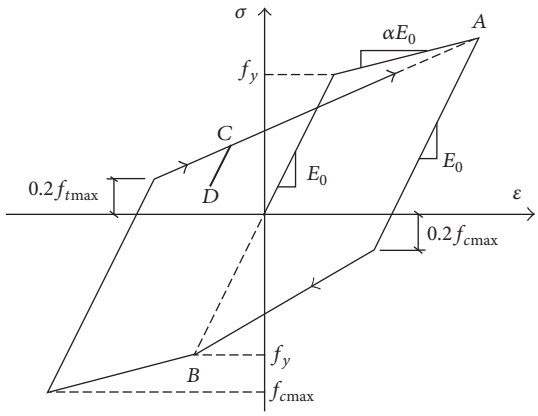

Figure 4: USTEEL02 rebar model [7].

the basis of the maximum point-oriented bilinear model proposed by Clough [6] (see Figure 3), which could comprehensively consider the Bauschinger effect generated during the loading-unloading-reserve loading of rebar. Besides, its feasibility has been verified [30, 31]. The Bauschinger effect on the rebar can be taken into consideration by importing the subprogram into ABAQUS.

As shown in Figure 4, the USTEEL02 model comprises four material parameters: the elastic modulus, initial yield strength, stiffness coefficient after yielding, and the ultimate plastic deformation rate; it also includes 11 state variables. Meanwhile, it considers the postyield stiffness degradation of the rebar and flexural strength degeneration of members caused by cumulative damage, including the influence of hysteresis on factors such as concrete strength and stirrup ratio. Moreover, the downtrend of the skeleton curve after member failure is considered. The parameters in the model can be determined by using [7]

$$\alpha = \frac{E_y}{E_0};$$
$$\delta = \frac{\varepsilon_f E_0}{f_y}; \quad (2)$$
$$\varepsilon_f = \frac{0.15\lambda_V}{\mu},$$

where α is the postyield stiffness coefficient of the rebar (suggested value: 0.001); E_0 is the elastic modulus of the rebar; E_y is the postyield stiffness of the rebar; f_y is the yield strength of the rebar; δ is the plastic deformation rate; ε_f is the plastic deformation; λ_V is a hoop reinforcement property; and μ is the axial compression ratio.

2.2.2. The Reduction of Geometric Parameters and Degradation of Mechanical Properties of Rebar under Attack from Corrosion. In the atmosphere, the corrosion of rebar in RC structures is mainly caused by carbonisation, cracking, and spalling of the concrete cover. It can be assumed that the corrosion is uniform. As there are many corrosion products, such as rust, on the surface of the rebar during corrosion, the geometric parameters of the rebar, including its linear mass and effective cross-sectional area and its mechanical properties, such as yield strength, can be reduced to some extent. Although the corrosion of rebar is discrete, to a certain extent, the related model for the decline in yield strength and elastic modulus of rebar can be obtained through statistical analysis of multiple experiments [32]. Yuan et al. [10] provided a yield degradation model based on multiple tests on corroded rebar and found that

$$f_{yc} = f_{y0}\left(1 - 2.9\eta\right), \quad 0 < \eta \le 5\%,$$
$$f_{yc} = f_{y0}\left(1.175 - 6.4\eta\right), \quad \eta > 5\%, \quad (3)$$

where f_{yc} and f_{y0} are, respectively, the yield strength of rebar before and after corrosion and η stands for the corrosion rate of the cross-section [10].

As for actual RC structures and members, if the concentration of external harmful media, such as chlorides and sulphates, is high, besides, the mass of concrete being inhomogeneous and variable, the invasion time of the harmful media to the rebar will vary. Inevitably, the corrosion time for rebar is different; that is to say, nonuniform corrosion occurs. In addition, the nonuniformity is more significant with increasing corrosion which induces local pitting corrosion on the rebar which can lead to stress concentration and a further reduction in the bearing capacity of structures and members. The yield strength reduction of rebar under the effects of pitting corrosion can be computed by the following formula [33]:

$$f_y(t) = \left(1 - \alpha_y \eta_{\text{pit}}\right) f_{y0}, \quad (4)$$

where $f_y(t)$ is the yield strength after corrosion of the rebar; α_y is an empirical coefficient (suggested value: 0.005); η_{pit} is the corrosion rate of the pitting-corroded cross-section; and f_{y0} is the yield strength of the rebar before corrosion.

With respect to the influence of corrosion on the elastic modulus of the rebar, some researchers find that the elastic modulus of rebar changed little with increasing corrosion rate [34]. When the corrosion is uneven, Lee et al. [35] found that the corrosion of rebar can weaken its elastic modulus as given below:

$$E_{sx} = \left(1 - 0.0113\eta_m\right) E_s, \quad (5)$$

where E_{sx} is the elastic modulus of the rebar after corrosion; η_m is mass loss rate due to rebar corrosion; and E_s is the elastic modulus of the rebar before corrosion. The transform relationship between the cross-sectional loss rate in a pitting-corroded rebar and the mass loss rate [36] is given by

$$\eta_s = \begin{cases} \eta_m, & 0 \le \eta_m < 2\%, \\ 0.015 + 0.97\eta_m, & 2\% \le \eta_m < 10\%, \\ 0.062 + 0.95\eta_m, & 10\% < \eta_m \le 20\%, \end{cases} \quad (6)$$

where η_s is the cross-sectional loss rate and η_m the mass loss rate.

For analysis, the rebar model can be reasonably simplified. (1) Assuming that the corrosion rates of stirrups and the main longitudinal reinforcement are the same and that the constraining effects of the stirrups on the core concrete are ignored, the beneficial effect of any stirrups can be neglected owing to the stirrup ratio of general RC members being low and the constraint of stirrups on the core concrete being slight. (2) As for the local nonuniform pitting corrosion of longitudinal reinforcement, the shape and distribution of pitted zones are random. If the finite element model is established according to the actual shape and distribution of these pitted zones, the modelling computational effort becomes large, while the computational efficiency decreases. Some researchers have studied the influence characteristics of pitting corrosion on RC members under uniform corrosion. Besides, they provided a conversion formula between local pitting corrosion and uniform corrosion [34] (see (7)). Thereby, the transform relation was used during this research. In addition, a uniform corrosion was used to simulate pitting corrosion of the longitudinal reinforcement

$$R = \frac{p(t)}{p_{\text{av}}(t)}. \quad (7)$$

In (7), $p(t)$ is the maximum pit depth; $p_{\text{av}}(t)$ is the average pit depth; and R is a pitting coefficient (suggested value $5 \le R \le 13$) [34].

2.3. Bond-Slip Constitutive Relationship. There is relative slippage between concrete and rebar, when RC members are subjected to low frequency cyclic loading. To some extent, slippage can absorb the energy in members produced by external loads. One of the macro-behaviours is a pinch effect caused by hysteresis. The bond-slip stress between concrete and rebar mainly originates from friction, cohesive forces from the cement material on the rebar, and the mechanical interaction between the surface of the deformed rebar and the concrete before corrosion. The surface roughness of the rebar decreased and some threads on the surface were lost: this affected the stick-slip behaviour after corrosion of the rebar.

The relative slippage between concrete and rebar could be simulated by defining a nonlinear spring element in ABAQUS. Owing to load being added to the top side of the frame column during simulation, slippage of the rebar mainly appeared along the longitudinal column axis (the Z-direction), while horizontal, X-, and Y- directions slippage was negligible. That is to say, two linear spring elements with larger stiffness (2×10^{11} to 2×10^{13} N/mm) were set on the overlapped nodes of the concrete and rebar in the X- and Y-directions, and a nonlinear spring element was used in the Z-direction. The force-displacement relationship of the nonlinear spring element is given by [33]

$$F = \tau(D) A_i, \quad (8)$$

where $\tau(D)$ is the shear stress in bond-slip and A_i is the distribution area across the corresponding contact surface of the spring.

According to the experience of the authors, the calculation mode of slippage-induced shear stress-displacement, as defined by CEB-FIB MODEL CODE 1990 [37], was applied to determine the shear stress governing bond-slip. In this way, the bond-slip force between the rebar and concrete was modelled. In addition, the mode was characterised by few parameters and a simple calculation [38]:

$$\beta = \begin{cases} 1 + 0.9943\eta_s - 0.9584{\eta_s}^2 + 0.3461{\eta_s}^3 - 0.0447{\eta_s}^4, & \eta_s \le 3\%, \\ 1.4822{\eta_s}^{-0.4235}, & \eta_s > 3\%, \end{cases} \quad (9)$$

where β is the reduction coefficient for the ultimate bond strength and η_s is the rebar corrosion rate.

3. Establishment of the Finite Element Model

3.1. Model Parameters. To compare with existing results [13], a frame column was simulated. The cross-section measured 200 × 200 mm, and the section of the foundation beam was a rectangle measuring 250 × 300 mm. In addition, the concrete cover thickness was 25 mm. The longitudinal reinforcement was Grade II rebar (symmetrical), while Grade I rebar was used for the stirrups. Moreover, the design strength grade was chosen as a C25 grade concrete. Figure 5 shows the geometric parameters and the reinforcement layout. The bottom of the column was fixed. During testing, a vertical jack was used to increase the load to 325.08 kN. It was calculated that the axial compression ratio of the column was 0.27. In addition, the lateral repeated force was applied by a horizontal two-dimensional hydraulic jack sited some 100 mm below the top of the column. The measured concrete compressive strength of the mix used to form the frame column was 31.1 MPa and its tensile strength was approximately 4 MPa, and the initial elastic modulus and Poisson's ratio were approximately 30 GPa and 0.2, respectively (estimated values only). The measured yield strength of the longitudinal reinforcement in the column was 415.6 MPa and the elastic modulus was about 200 GPa before corrosion.

3.2. Finite Element Model and Loading Scheme. To consider the influence of corrosion on the bond-slip between the rebar and the concrete, discrete modelling was used, including C3D8R for concrete elements with a unit size of 100 × 25 × 25 mm and T3D2 for rebar with a unit size for longitudinal reinforcement and stirrups of 100 mm and 35 mm, respectively. Then a nonlinear spring constraint was imposed in the

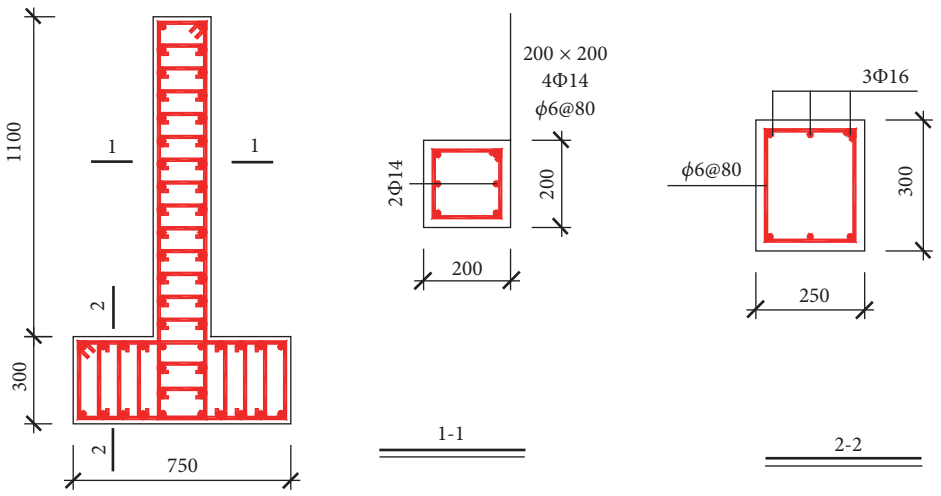

Figure 5: Dimensions and reinforcement layout.

longitudinal direction (the Z-axis). Besides, a linear spring constraint with a stiffness of 2×10^{12} N/mm was applied to the section orientation, that is to say, X- and Y-directions of the column to simulate bond-slip between the rebar and concrete. The established concrete model and framework model for the reinforcement are shown in Figure 6.

Owing to the bottom of frame column being fixed, a fixed constraint was applied at the nodes of grid at its base. A concentrated force of 325.08 kN was applied to simulate the axial compression. Reference point RP1 was established at 100 mm below the top surface of column and it was coupled with the top surface. The displacement loading method was adopted to simulate the effect of lateral repeated force. Cyclic loading was preformed according to displacement amplitudes $\Delta_y, 2\Delta_y, 3\Delta_y, \ldots$ with three loops *per* amplitude. Then the loading was stopped when the bearing capacity of frame column dropped to 85% of its ultimate loading capacity, among which $1.0\Delta_y, 1.5\Delta_y, 2.0\Delta_y, \ldots, \Delta_y$ were regarded as the yield displacement of the frame column.

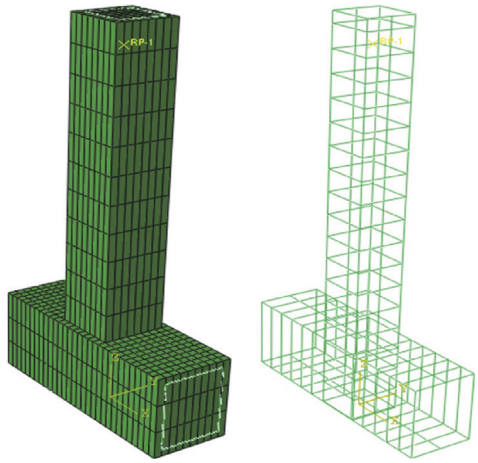

(a) Concrete model (b) Framework model of reinforcement

Figure 6: Finite element models for concrete and rebar.

4. Numerical Simulation and Analysis of the Hysteresis Performance of Corroded RC Frame Columns

4.1. Analysis of Load Cases and Calculation Parameters. To understand the influence of different amounts of rebar corrosion on the hysteresis performance of a frame column, four sets of operating conditions, including noncorroded, slight corrosion, moderate corrosion, and severe corrosion, along with the influence of local pitting corrosion, were selected. According to the literature [33], the corresponding corrosion rates for a pitting-corroded cross-section under the four conditions above were 0%, 6.3%, 25%, and 56.3%, respectively. Assuming that pitting corrosion coefficient $R = 5$, the corresponding uniform corrosion rates of the rebar cross-section were 0%, 5%, 10%, and 15%, respectively (obtained by (7)). The corresponding reinforcement parameters under the four load cases, including the yield strength of the rebar and the bond-slip degradation coefficient, are listed in Table 2.

4.2. Simulation Results and Analysis

4.2.1. Uniaxial Pushover Analysis. To obtain the yield displacements of each frame column under various corrosion conditions during loading, firstly a uniaxial pushover analysis was conducted on each frame column under different cases. The target displacement was set to 45 mm according to Chinese Standard GB50011-2010 (Code for the Seismic Design of Buildings) [39]. The results are shown in Figure 7.

As shown in Figure 7, under static displacement the corresponding peak bearing capacities under each case with different corrosion rates were as follows: 63 kN with a corrosion rate of 0%, 60 kN with a corrosion rate of 5%, 55 kN with a corrosion rate of 10%, and 49 kN with a corrosion rate

Table 2: Calculation parameters for different degrees of corrosion.

Corrosion rate (pitting corrosion rate)	0% (0%)	5% (6.3%)	10% (25.0%)	15% (56.3%)
Mass loss rate	0%	5.1%	10.5%	15.7%
Yield strength (MPa)	415.6	400.1	363.3	296.4
Elastic modulus (GPa)	200	197.7	176.3	164.5
Degradation coefficient of bond-slip	1.0	0.75	0.56	0.47

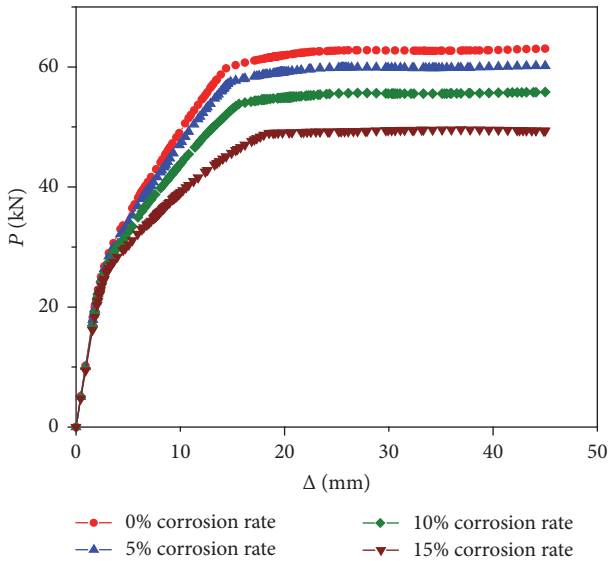

Figure 7: Uniaxial pushover analysis of frame columns with different corrosion rates.

of 15%. According to the PARK yield displacement principle [40], the yield displacements under cases with different corrosion rates were calculated as 10 mm with a 0% corrosion rate, 9.7 mm with a 5% corrosion rate, 8.8 mm with a 10% corrosion rate, and 7.6 mm with a 15% corrosion rate. It also can be seen that, with an increased corrosion rate, the static ultimate bearing capacity and the yield displacement of the frame column decreased after corrosion of the rebar. Compared with noncorroded columns, the static ultimate bearing capacities of columns after corrosion, respectively, fell by 4.8%, 12.7%, and 22.2%, which was linearly related to the increase of corrosion rate. This implied that the decrease of yield strength of the rebar, its elastic modulus, and section loss caused by corrosion were important factors affecting the weakening of the static bearing capacity of frame columns. Compared with the static bearing capacity, the yield displacement decreased more significantly with increasing corrosion rate. With increasing corrosion rate, the yield displacements were decreased by 5.9%, 14.1%, and 25.9%, respectively, and the rates of decrease were greater than the average cross-sectional rate of decrease and mass loss. Overall, the yield displacement and corrosion rate had a nonlinear relationship. This illustrated that the degradation of bond-slip behaviour between the rebar and the concrete plays a more important role in the weakening of the static bearing capacity of frame columns.

4.2.2. Hysteresis Curves. Based on the aforementioned parameters, low frequency cyclic loading and unloading were performed on frame columns under various load regimes. The comparison of simulated hysteresis curves with the experimental results [13] is shown in Figure 8.

The comparison of the FE simulated results and the experimental results shows that the simulated hysteresis curves are similar in shape to those obtained experimentally [13]. During cyclic loading, the hysteresis curve for the noncorroded column was plump and arcuate which implied that the seismic energy absorption was favourable. With an increasing rebar corrosion rate, the plumpness of the hysteresis loop decreased, while the shrinkage increased. In addition, the hysteresis curve changed to a reverse S-shape from an arcuate form so that the area within the hysteresis loop decreased, causing a severe "pinching" phenomenon. Moreover, with an increasing corrosion rate, the frequency of cyclic loading and the ultimate displacement decreased, as did the seismic energy absorption ability of the column. This suggested that rebar corrosion was an important factor affecting the seismic energy absorption ability of frame columns. With increasing corrosion, the energy dissipation capacity of the frame columns decreased, while their brittleness increased.

4.2.3. Skeleton Curves. Skeleton curves are obtained by connecting the ultimate loading points for each tension or compression load cycle, in the same direction, on the hysteresis curve successively. Skeleton curves describe the trajectory of the maximum peak horizontal force at each cyclic loading stage and reflect the changes in the stress and deformation of members at different stages. Therefore, skeleton curves are an important index for assessing the seismic performance of members or structures, as well as a significant basis for determining the feature points in the restoring force model for such members.

The skeleton curves of frame columns with different corrosion rates were extracted (see Figure 9). As shown in Figures 9(a) and 9(b), the numerical and experimental ultimate loads under each case with different corrosion rates were as follows: 52.3 and 50.15 kN with a corrosion rate of 0%, 47.9 and 49.65 kN with a corrosion rate of 5%, 44.8 and 49.5 kN with a corrosion rate of 10%, and 39.3 and 43.54 kN with a corrosion rate of 15%. It can be seen that the bearing capacity of the frame columns decreased with increasing rebar corrosion rate, and the numerical and experimental peak bearing capacities decreased by approximately 8.4%, 14.3%, and 24.9% and 1.0%, 1.3%, and 13.2%, respectively, during cyclic loading. Moreover, the larger the corrosion

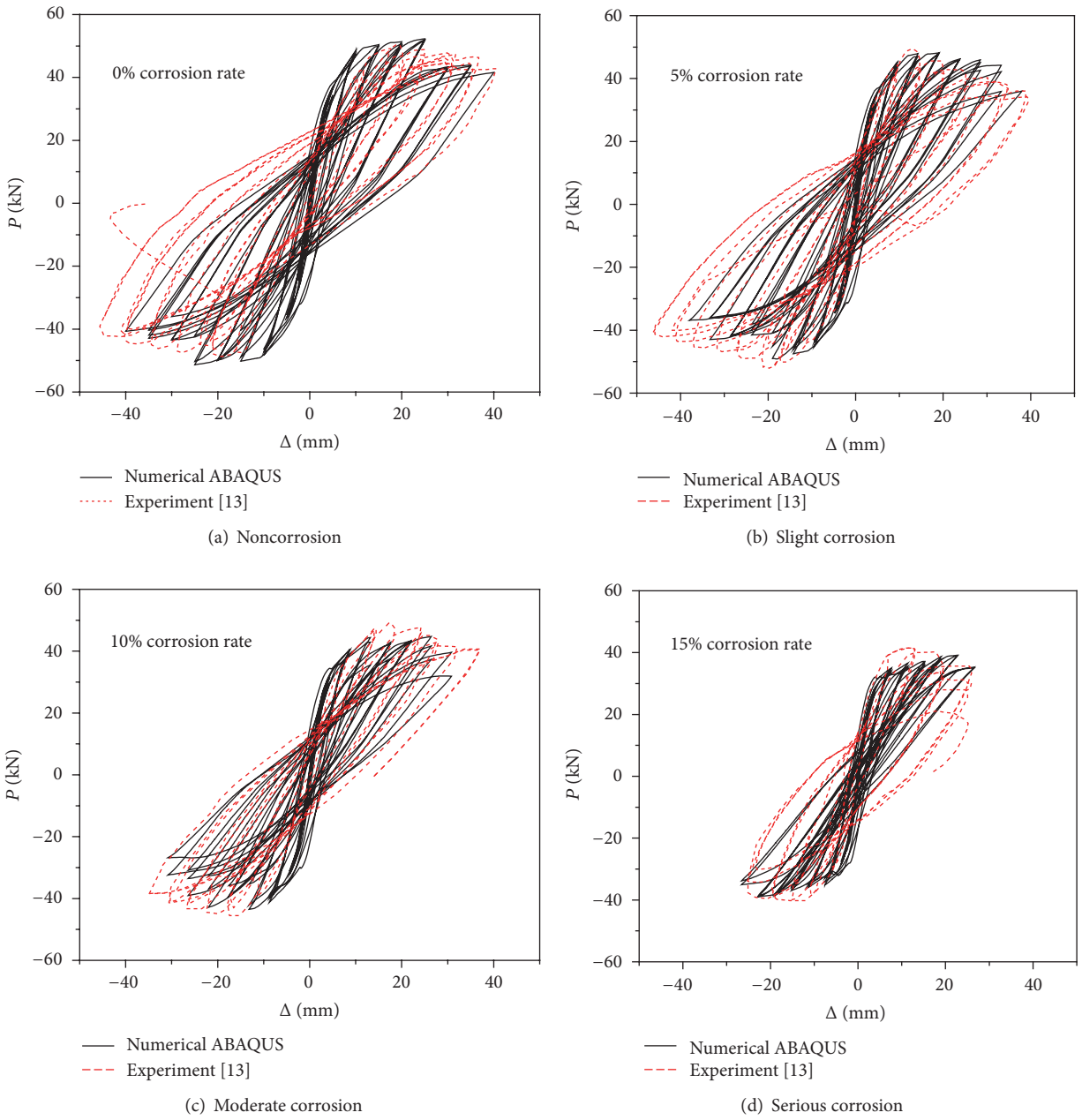

Figure 8: Hysteresis curves for RC columns under different corrosion rates.

rate, the greater the decrease in bearing capacity. Meanwhile, as the rebar corrosion rate increased, the rising segment of the skeleton curve was flattened and seen to have had a shortened strengthening segment, implying a weakened capacity to resist deformation, and a lower ductility of the frame columns.

It needs to be pointed out that the FE simulation results and experimental results in Figures 8 and 9 are not identical. This is mainly because there are various factors affecting the hysteretic performance of corroded RC frame columns. FE simulation cannot take all of these factors into account. In addition, the property, size, and reinforcement ratio of the concrete materials used in the tested samples are of larger-scale with regard to their discretisation. Moreover, the loading rate and constraint conditions in the experiment exert influences on the experimental results as well. In spite of this, the authors believe that it is feasible to study the hysteresis performance of corroded RC frame columns using a FE numerical simulation.

Based on the above analysis, the following suggestions can be applied to the seismic reinforcement of corroded RC frame columns: for mildly corroded members (i.e., those with a rebar corrosion rate within 5%) whose hysteretic bearing capacity reduces slightly to within 10%, then such structures, or members, can be slightly, or non-, reinforced according to their importance in engineering practice. Regarding the

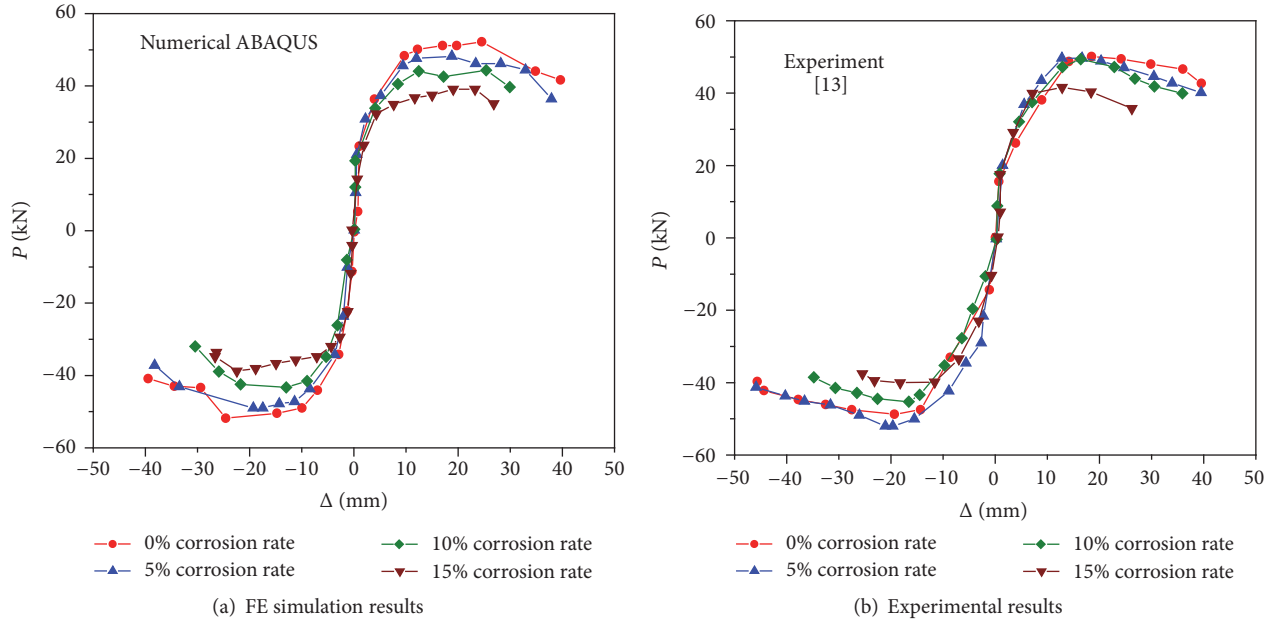

(a) FE simulation results

(b) Experimental results

Figure 9: Skeleton curves for RC columns under different corrosion rates.

slightly corroded members with corrosion rates of 5% to 10%, their hysteretic bearing capacity was reduced by 10% to 20%, indicating that members were in a poor state. Therefore, such members are expected to be reasonably reinforced. Owing to the hysteretic bearing capacity of moderately corroded members (with corrosion rates of between 10% and 15%) decreased by 20% to 30%, the members need to be given more attention when designing/assessing their reinforcement as they are in poorer condition. In view of the more seriously corroded members, the corrosion rate of which is above 15%, their hysteretic bearing capacity decreases significantly (by more than 30% generally), indicating there is an increased risk from such members. Thereby, these kinds of members should be replaced.

4.2.4. Deformation and Failure Characteristics. To understand the final deformation and failure characteristics of corroded frame columns under cyclic loading, the stress distributions and deformed shapes of each column were extracted. Figure 10 shows the stress distributions and deformations of frame columns with different corrosion rates. It can be seen that these frame columns presented similar deformation characteristics under various operating conditions. The key difference was that the deformation became more severe as the corrosion rate increased.

Figure 11 shows seismic damage to RC columns: the deformation of such frame columns in a numerical simulation under cyclic loading was consistent with that of the column after an actual earthquake (see Figures 10 and 11). The concrete at the bottom of both columns was crushed and the rebar was bent into a cage. This indicated that the numerical simulation results for the hysteresis performance of a corroded frame column can well reflect their damage characteristics in a real earthquake.

5. Restoring Force Model of a Corroded RC Frame Column

5.1. Selection of the Restoring Force Model. In the seismic response analysis of structures, the actual hysteresis performance curves are commonly modelled (using the restoring force model). For RC structures, the restoring force model is generally divided into two levels. The first level is the restoring force model of the materials used: this is mainly designed to reveal the stress-strain relationship between rebar and concrete and is the basis for modelling the restoring forces in RC members. The second level is the restoring force model of the members, which is used to describe the hysteretic relationship between bending moment and curvature (M-Φ) in the beam sections and that between the load and displacement (P-Δ) of columns. Since the first has been extensively studied with well-acknowledged conclusions, the authors merely considered the restoring force model on a member level.

A suitable restoring force model for RC members needs to meet the following two requirements simultaneously: firstly, the model is expected to exhibit a certain precision, reflect the hysteretic performance of actual structures or members, and replicate experimental results within an acceptable tolerance through numerical simulation. Secondly, the model should be simple and practical, so that it does not present unnecessary complexity which hinders the effective performance of static elastoplastic, or dynamic nonlinear time-history, analysis.

In earthquakes, when RC structures are subjected to elastoplastic stress stages, the plastic deformation of structures can absorb large amounts of the input energy, which endows the relationship between the restoring force and displacement of members with apparent hysteretic nonlinearity. Considering this characteristic, the restoring force model for

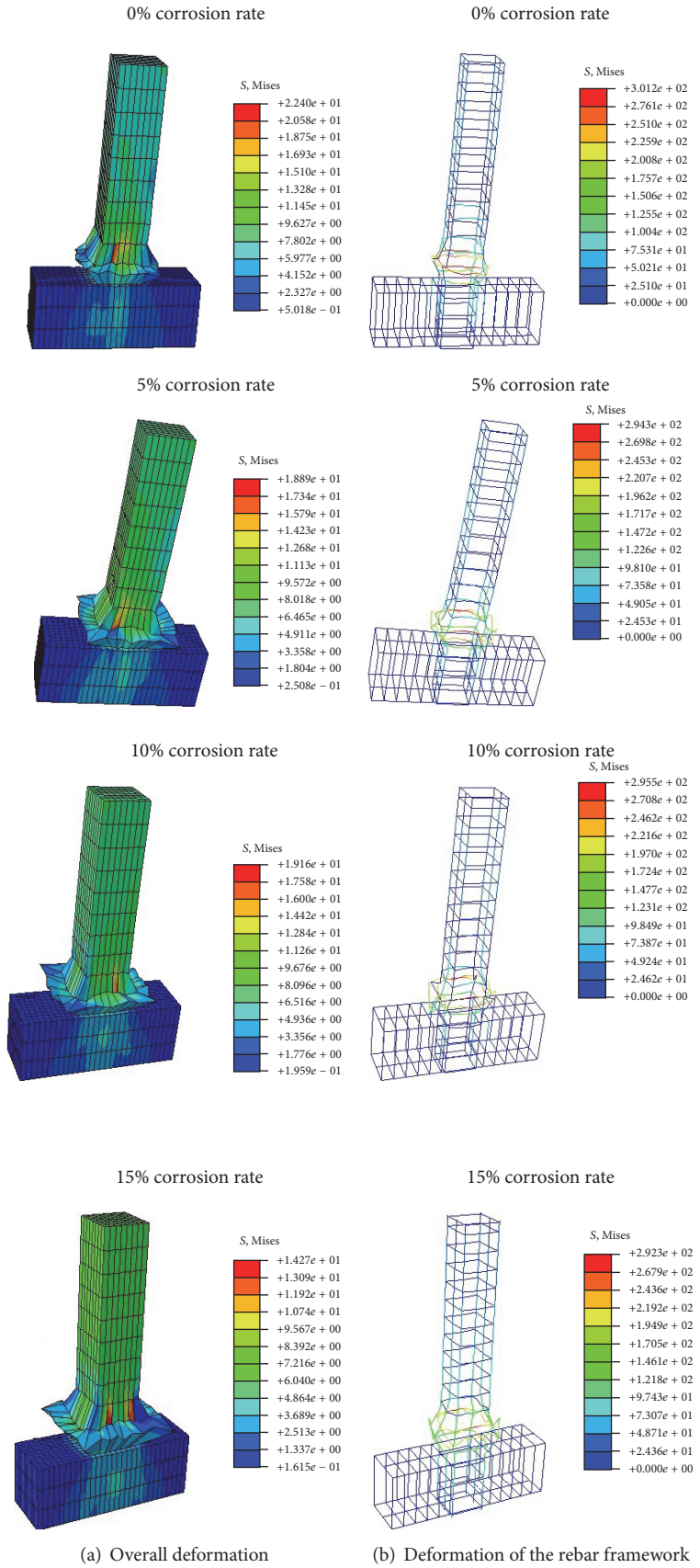

(a) Overall deformation (b) Deformation of the rebar framework

Figure 10: The stress, and final deformation, of corroded frame columns under cyclic loading.

Figure 11: Seismic damage to RC columns.

describing actual RC structures and members is divided into two types with curves and polygonal lines. The curvilinear restoring force model describes the actual stress characteristics of structures more accurately. However, its computations are complex, and the model is thereby rarely applied. As for that using polygonal lines, although it is comprised of several line segments and demonstrates a discontinuous stiffness distribution and has inflection points, it can be used without undue difficulty. Therefore, the restoring force model with polygonal lines has become widely used in practice.

The simplest nonlinear hysteretic model is bilinear elastoplastic model. Its positive loaded skeleton curve is composed of two lines and its shape is determined by yield strength, elastic stiffness, and postyield stiffness of members. As to the negative loaded skeleton curve, its loading and unloading stiffness are constant and equal to the elastic stiffness, which is similar to the positive loaded one. However, one of the shortcomings of this model is the difficulty of accounting for the stiffness deterioration of RC elements during cyclic load reversals. To overcome the problem of stiffness deterioration, Clough [6] proposed a model, which can consider the stiffness degradation of RC members under cyclic loading at nonlinear stage. Both bilinear and Clough models are simple to be applied, while they are merely suitable for members under simple bending with spindle hysteresis curves. Hence, several enhancements were done to these models in order to better simulate different characteristics of RC members. In 1970, a more refined and sophisticated hysteresis model was developed by Takeda et al. [41] on the basis of experimental results. In this model the monotonic behaviour is described by a trilinear skeleton curve which accounts for flexural cracking of concrete and yielding of reinforcing steel and also strain-hardening characteristics. The unloading stiffness was reduced by an exponential function of the previous maximum deformation. However, the Takeda model, similar to the Clough model, simulates dominantly flexural behaviour. Subsequently, a variety of improved hysteretic models emerged one after another.

To verify the effect of different hysteretic models on the dynamic response of RC frames, Anderson and Townsend [42] used four different models to describe the hysteretic behaviour of critical regions of RC members. The study shows that the most representative and practical model is the degrading trilinear (D-TRI) model. The D-TRI model uses three lines to describe the loading and restoring force skeleton curve and considers the stiffness degradation properties of an RC structure or structural component. The model can describe in more detail the cracking and yield of concrete and complex hysteresis rules. Therefore, it can preferably illustrate the relationship between the restoring force and deformation of concrete structures and members in the whole process. Due to this advantage, the D-TRI model is the most commonly used in the analysis of the elastoplastic seismic response of RC structures.

Based on the above analysis, we use the D-TRI model to investigate the hysteresis performance of RC frame columns in this paper. The skeleton curve and basic hysteresis rule of D-TRI model are shown in Figure 12. The skeleton curve was determined by parameters including yield load P_y, yield displacement Δ_y, ultimate load P_u, peak displacement Δ_u, failure load P_{cu}, and failure displacement Δ_{cu}. The modified Clough model, that is, the maximum historical displacement-oriented model, was adopted as the basic hysteretic rule here. The loading was conducted in numerical order [43, 44], as shown in Figure 12(b).

In Figure 12, K_y is the initial elastic stiffness, K_u is the postyield stiffness, and K_{cu} is softening stiffness. When the horizontal seismic force exceeded the yield loading P_y or the seismic displacement was greater than the yield displacement Δ_y, it was a strengthening process, while once the force reached the ultimate load, it became a softening process.

Once the key points of the bearing capacity and displacement were determined on the skeleton curve in the D-TRI model, the values of K_y, K_u, and K_{cu} can be calculated as follows:

$$K_y = \frac{P_y}{\Delta_y},$$

$$K_u = \frac{\left(P_u - P_y\right)}{\left(\Delta_u - \Delta_y\right)}, \tag{10}$$

$$K_{cu} = \frac{\left(P_{cu} - P_u\right)}{\left(\Delta_{cu} - \Delta_u\right)}.$$

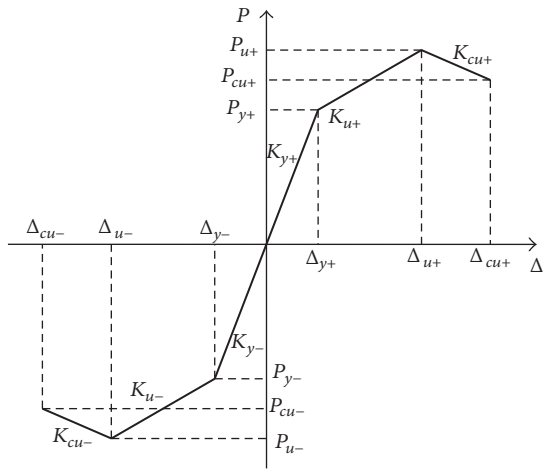

(a) Skeleton curve: D-TRI model

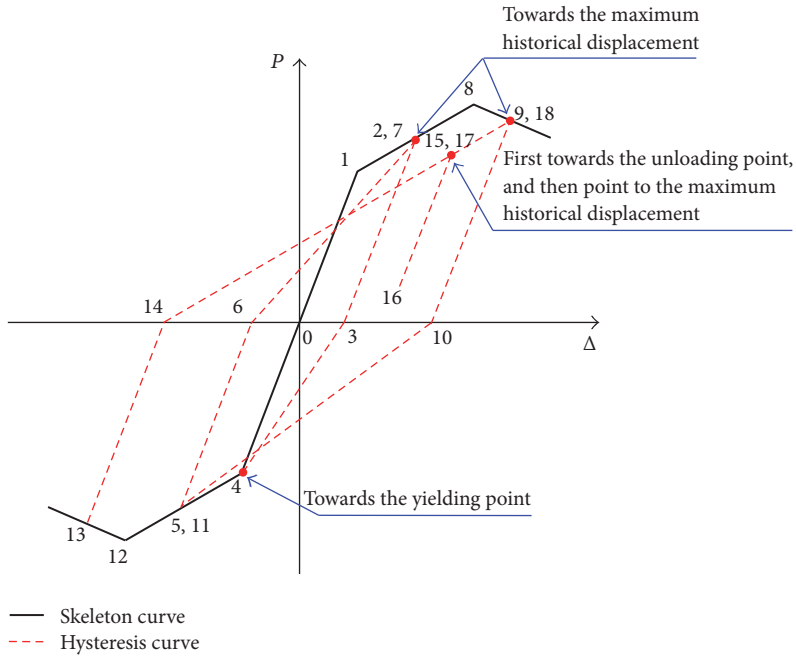

(b) Basic hysteresis rule: D-TRI model

Figure 12: D-TRI model.

After determining the above parameters, the formula for the restoring force model of members can be established. Furthermore, owing to symmetrical reinforcement being generally applied to RC frame columns in practice, the hysteresis curve is basically central-symmetric under cyclic loading. Therefore, to simplify the computation, it was assumed that the restoring force model was central-symmetric, that is, $P_{y+} = P_{y-}$ and $\Delta_{y+} = \Delta_{y-}$.

For corroded RC frame columns, it can be seen from Section 4.2 that the hysteresis curves and skeleton curves of corroded members exhibited basically identical shapes to those of noncorroded members under low frequency cyclic loading. The difference was that when influenced by rebar corrosion, the parameters depicting the characteristics of the restoring force decreased. Meanwhile, as seen in Figure 9, the trends for the skeleton curves of corroded, and noncorroded, members were basically consistent and roughly corresponded to the features of a trilinear equivalent model. The difference lays in the different coordinates of the feature points of bearing capacity and displacement of members.

Based on the above analysis, it was assumed that corroded and noncorroded members had similar restoring force models: therefore D-TRI model was applicable to both kinds of members, as displayed in Figure 13. In this way, (10) were used to compute key parameters in the restoring force model for noncorroded columns. Then, the parameter values of

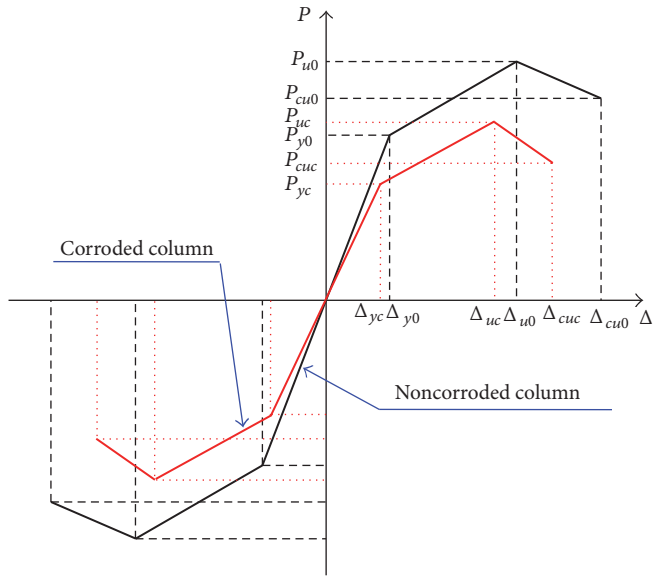

FIGURE 13: Skeleton curves for D-TRI model of corroded, and noncorroded, columns.

the key points on the skeleton curve for the restoring force model of corroded columns were obtained by introducing the corrosion-induced reduction coefficient of the mechanical performance index of frame columns.

5.2. Determining Key Parameters of the Skeleton Curve for the Restoring Force Model

5.2.1. Determining Key Parameters for Noncorroded Members. The determination of the feature point parameters of the skeleton curve for the restoring force model of a noncorroded RC column played a fundamental role in establishing the restoring force model for corroded ones.

(1) Yield Load P_{y0} and Yield Displacement Δ_{y0}. Yield load P_{y0} is defined as the corresponding horizontal thrust when tensile rebar yields at the maximum bending moment section; the corresponding bending moment is the yield moment M_{y0}. According to plane cross-section assumptions, it can be found that the relationship between yield load P_{y0} and bending moment M_{y0} is

$$P_{y0} = \frac{2M_{y0}}{H_0}, \tag{11}$$

where H_0 is the height from the horizontal loading point of the frame column to the column base and M_{y0} is the yield moment of the cross-section, which can be calculated on the basis of [45]

$$\begin{aligned} M_{y0} &= A_{s0} f_{y0} (h_0 - a) + n_0 b h_0 f_{c0} \left(\frac{h}{2} - a\right) \\ &\quad - 0.5\kappa b h_0 f'_{c0} \left(\frac{\kappa h_0}{3} - a\right), \\ f'_{c0} &= \frac{\kappa f_{y0}}{(1-\kappa)\alpha_E}, \\ \alpha_E &= \frac{E_s}{E_c}, \end{aligned} \tag{12}$$

where A_{s0} is the tensile longitudinal reinforcement area; f_{y0} is the design yield strength of the longitudinal reinforcement; h_0 is the effective height of the cross-section of the member; h is the height of the cross-section of the member; b is the width of the cross-section of the member; a is the distance from the centre of the main tension reinforcement to the edge of the cross-section; n_0 is the axial compression ratio; f_{c0} is the measured strength of the concrete [46]; κ is the relative height of the compression zone; f'_{c0} is the stress in the concrete on a cross-section when the tensile rebar yields, where $f'_{c0} > f_{c0}$, setting $f'_{c0} = f_{c0}$; E_s is the elastic modulus of the rebar; and E_c is the measured elastic modulus of concrete [46].

The relative height of the compression zone κ is given by [45]

$$\begin{aligned} \kappa &= \left\{\left(\rho_t + \frac{n_0}{\alpha_f}\right)^2 \alpha_E^2 + \left[\rho_t\left(1 + \frac{a}{h_0}\right) + \frac{2n_0}{\alpha_f}\right]\alpha_E\right\}^{0.5} \\ &\quad - \left(\rho_t + \frac{n_0}{\alpha_f}\right)\alpha_E, \end{aligned} \tag{13}$$

where $\alpha_f = f_{y0}/f_{c0}$; ρ_t is the reinforcement ratio of the main tension reinforcement.

As the stiffness degradation is not obvious from concrete cracking to rebar yielding in actual frame columns, the member is assumed to be perfectly elastic before rebar yielding. Therefore, the yield displacement Δ_{y0} [45] is

$$\Delta_{y0} = \frac{H_0^2 f_y}{3h_0 (1-\kappa) E_s}. \tag{14}$$

(2) Ultimate Load P_{u0} and Peak Displacement Δ_{u0}. By regression analysis on the obtained data [47], the ultimate load was given by

$$P_{u0} = (1.24 - 0.075\rho_t n_0 - 0.5 n_0) P_{y0}. \tag{15}$$

Table 3: Calculated results of yield load (P_y) and yield displacement (Δ_y) and those obtained through FE simulation and experiments.

Corrosion rate (%)	Formula (*a*)	Numerical ABAQUS (*b*)	Experiment [13] (*c*)	Relative error (%) ((*a*) − (*c*)/(*c*)) × 100%
			Yield load P_y (kN)	
0	47.6	49.0	41.78	13.9
5	43.8	45.0	41.15	6.4
10	39.3	40.5	42.05	−6.5
15	34.0	35.0	37.11	−8.4
			Yield displacement Δ_y (mm)	
0	9.8	10.0	9.32	5.2
5	9.7	9.7	9.36	3.6
10	9.2	8.8	10.84	–15.1
15	8.2	7.6	7.85	4.5

Considering the influence on the mechanical properties of the members of factors such as the properties of the concrete, axial compression ratio, and shear span ratio, during the determination of peak displacement, an empirical method was used to fit the calculated data to obtain an expression for the peak displacement [47]:

$$\Delta_{u0} = \frac{1}{0.045 + 1.75n_0}. \tag{16}$$

(3) Failure Load P_{cu0} and Failure Displacement Δ_{cu0}. In general, if the bearing capacity of RC members was reduced to 85% of the ultimate load, the structural, or member, failure was determined as a failure during testing; namely,

$$P_{cu0} = 0.85P_{u0}. \tag{17}$$

The corresponding displacement to failure load P_{cu0} was a failure displacement Δ_{cu0}. On the basis of the statistical analysis of simulated data [47], the effect of factors, including the properties of the concrete, axial compression ratio, reinforcement ratio of tensile reinforcement, and section size, was taken into account to determine the calculation method of failure displacement as

$$\Delta_{cu0} = (5.20 - 4.1n_0)\,\Delta_{y0}. \tag{18}$$

5.2.2. Determining Key Parameters for Corroded Members. Rebar corrosion can induce a decrease in the cross-sectional area thereof, as well as its yield strength, bond behaviour, ultimate elongation, and so forth. Besides, there are many coupled factors which could interact: generally, corrosion degradation parameters are usually related to the axial compression ratio n_0 and corrosion rate η_s. Hence, the key parameters for a corroded member were established by analysing and fitting the data [47]:

(1) Yield load P_{yc} and yield displacement Δ_{yc}:

$$\begin{aligned} P_{yc} &= \left[0.9993 - 0.0531\eta_s n_0 - 0.0043\left(\eta_s n_0\right)^2\right] P_{y0}, \\ \Delta_{yc} &= \left[1.0015 + 0.01\eta_s n_0 - 0.0123\left(\eta_s n_0\right)^2\right] \Delta_{y0}. \end{aligned} \tag{19}$$

(2) Ultimate load P_{uc} and peak displacement Δ_{uc}:

$$\begin{aligned} P_{uc} &= \left[0.9964 - 0.0475\eta_s n_0 + 0.003\left(\eta_s n_0\right)^2\right] P_{y0}, \\ \Delta_{uc} &= \mu_{u0}\Delta_{yc}. \end{aligned} \tag{20}$$

(3) Failure load P_{cuc} and failure displacement Δ_{cuc}:

$$\begin{aligned} P_{cuc} &= 0.85P_{uc}, \\ \Delta_{cuc} &= \left[0.9871 - 0.0818\eta_s n_0\right] \Delta_{cu0}. \end{aligned} \tag{21}$$

For noncorroded and corroded members, the corresponding stiffness parameters can be acquired by substituting the bearing capacity and key displacement parameters on the skeleton curve, respectively.

5.3. Verifying the Reliability of the Restoring Force Model

5.3.1. Verifying the Accuracy of Key-Point Parameters of the Skeleton Curve. The parameters for each member in Section 3.1, such as material property parameters, axial compression ratio, and corrosion ratio, were substituted into (11) to (21). By doing so, the authors compared the calculated, FE simulated, and experimental results for key-point parameters of the skeleton curve for the restoring force model, as shown in Tables 3–5. It can be seen that the computed key-point parameters of the skeleton curve for the restoring force model of the corroded frame columns were generally consistent with those acquired in FE simulation and experiments [13]. Except for a few data points with large discrepancies with the experimental results (of up to 25%), most of the discrepancies were within 15%. This indicated that the proposed formulas for fitting the key-point parameters of the skeleton curve were reasonable.

5.3.2. Validation of the Accuracy of the Skeleton, and Hysteresis, Curves. The calculated key-point parameters of skeleton curve for the restoring force model in Section 5.3.1 were substituted into (10). Then according to the basic hysteresis rule shown in Figure 12(b), the skeleton, and hysteresis,

Table 4: Computed results of ultimate load P_u and peak displacement Δ_u and those acquired by FE simulation and experiments.

Corrosion rate (%)	Formula (a)	Numerical ABAQUS (b)	Experiment [13] (c)	Relative error (%) $((a) - (c)/(c)) \times 100\%$
			Ultimate load P_u (kN)	
0	52.2	52.3	50.15	4.1%
5	49.0	47.9	49.65	−1.3%
10	46.5	44.8	49.5	−6.1%
15	44.5	39.3	43.54	2.2%
			Peak displacement Δ_u (mm)	
0	23.6	24.5	22.54	4.7
5	22.9	18.3	22.37	2.4
10	20.8	25.9	19.75	5.3
15	17.9	22.4	14.32	25.0

Table 5: Calculated results of failure load P_{cu} and failure displacement Δ_{cu} and those obtained in FE simulation and experiments.

Corrosion rate (%)	Formula (a)	Numerical ABAQUS (b)	Experiment [13] (c)	Relative error (%) $((a) - (c)/(c)) \times 100\%$
			Failure load P_{cu} (kN)	
0	44.4	42.5	42.63	4.2
5	41.7	43.6	42.2	−1.2
10	39.5	40.2	42.07	−6.1
15	37.8	35.3	37.01	2.1
			Failure displacement Δ_{cu} (mm)	
0	40.9	39.5	41.54	3.4
5	35.9	34.0	39.51	−9.1
10	31.3	30.0	32.52	−3.8
15	26.8	26.3	24.1	11.2

curves of the corroded frame columns with their different corrosion rates were obtained, as shown in Figure 14.

From Figure 14, it could be seen that the hysteresis curves and skeleton curves of the restoring force model obtained by fitting formulas were generally consistent with those obtained in the experiment: with the increased rate of corrosion, the bearing capacity and the area within the hysteresis loop of the frame column decreased. This implied that the seismic energy dissipation capacity of the corroded frame columns decreased, while their brittleness increased. These results validated the idea that numerical simulation would be a simple, feasible method of constructing the restoring force model of corroded RC members: the established model was found to have been accurate and was deemed reasonable.

6. Conclusions

ABAQUS finite element software was used for the numerical simulation analysis of the hysteresis performance of RC frame columns with four different amounts of corrosion: non-corroded, slight corrosion, moderate corrosion, and severe corrosion. In addition, the analytical results were compared with published experimental results and actual earthquake damage characteristics of framed columns. On this basis, a D-TRI model was established to reflect the hysteresis performance of corroded RC frame columns. Moreover, the influence of factors including the rebar corrosion rate and axial compression ratio was taken into consideration. The main conclusions were as follows:

(1) The seismic bearing capacity of a frame column would be significantly decreased after corrosion of its rebar. In addition, with increasing rebar corrosion rate, the diminution of the bearing capacity gradually increased, including the corrosion-induced degradation of the bond-slip behaviour between rebar and concrete, which played an important role in weakening the hysteretic bearing capacity.

(2) Along with the increased amount of rebar corrosion, the plumpness of the hysteresis loop of a frame column decreased, while the shrinkage increased. Meanwhile, the hysteresis curve became a reverse S-shape, having originally been arcuate. Furthermore, the area within the hysteresis loop became smaller and generated severe "pinching": this explained why the seismic energy dissipation capacity of such frame columns decreased, while their brittleness increased.

(3) The FE simulated frame column showed failure and deformations similar to those experiencing actual earthquakes under cyclic loading. This suggested that it was feasible to simulate the hysteresis performance of corroded RC frame columns using

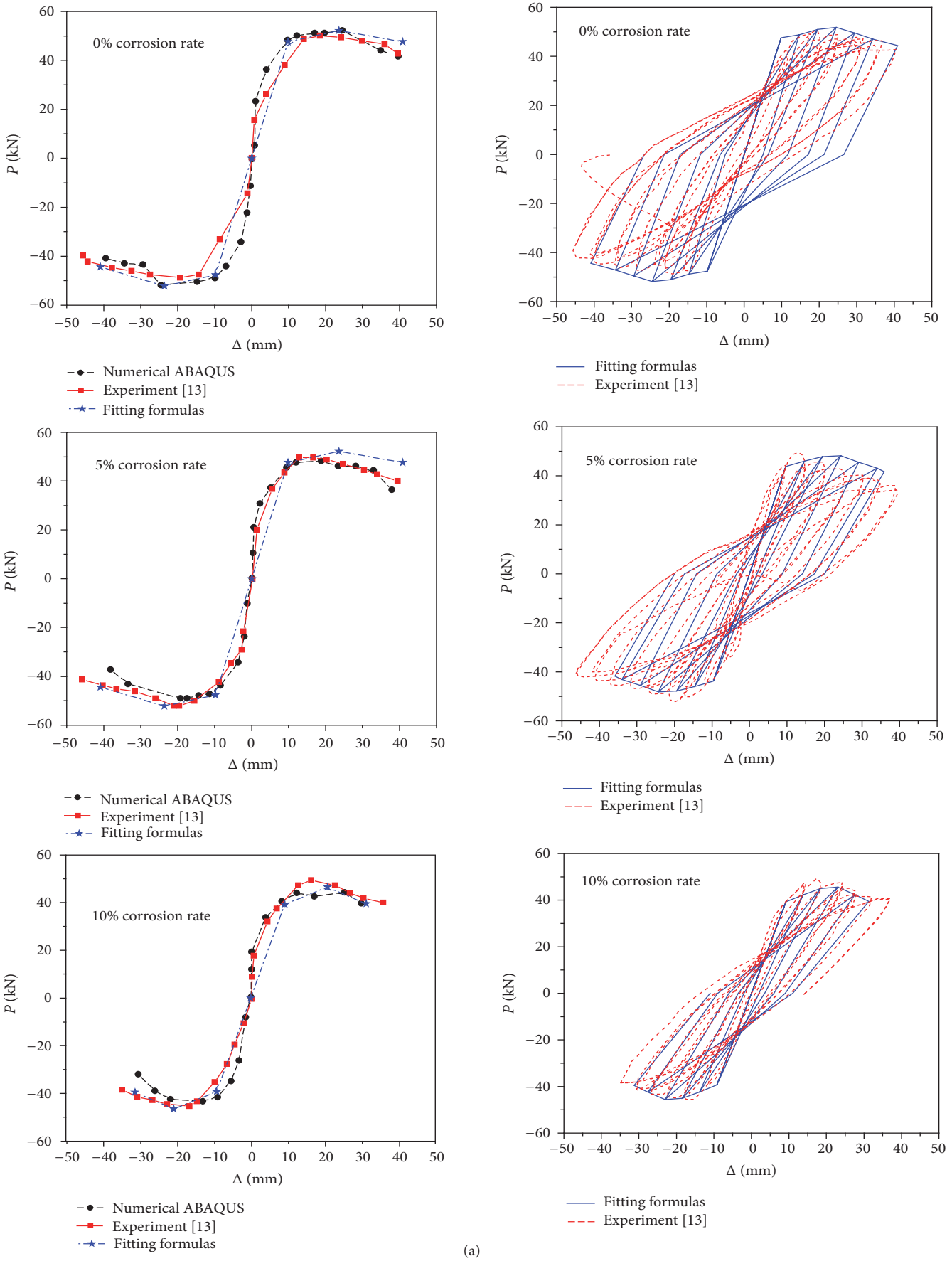

(a)

Figure 14: Continued.

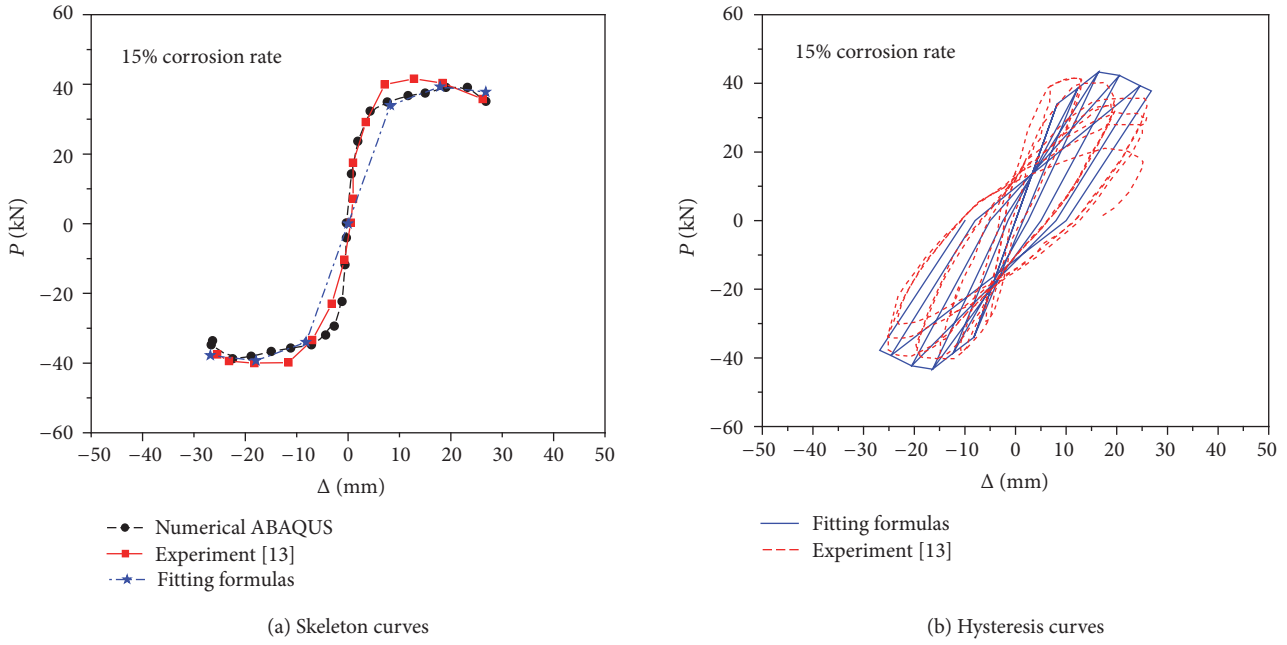

(b)

Figure 14: Comparison of skeleton curves and hysteresis curves obtained by the restoring force model and experiment.

the FE method. Furthermore, the simulated results favourably described the failure characteristics of the frame column in earthquake conditions.

(4) The hysteresis, and skeleton, curves of the corroded RC frame column presented basically consistent shapes with those of a noncorroded member under low-cyclic loading, which broadly conformed to the characteristics of a trilinear distribution. Therefore, a restoring force model applicable to corroded RC frame columns, the D-TRI restoring force model, for instance, could be established based on that of noncorroded RC members using the existing Clough hysteresis rule.

(5) The skeleton, and hysteresis, curves of corroded RC frame columns, predicted using the D-TRI model, were similar to those from experimental results. Except for a few data points which showed large discrepancies (25%) with the experimental results, most of the calculated key-point parameters of the skeleton curve presented discrepancies of less than 15%. Moreover, the hysteresis curve showed similar characteristics to the experimental results. This proved that the restoring force model established for the corroded RC members in this research using numerical simulation was simple and applicable, as well as accurate and rational.

Competing Interests

The authors declare that there is no conflict of interests regarding the publication of this paper.

Acknowledgments

This research has been funded by the National Natural Science Foundation of China (Grant nos. 51520105012 and 51278303) and Outstanding Young Talent Research Fund of Zhengzhou University (Grant no. 1521322004) and Guangdong Provincial Key Laboratory of Durability for Civil Engineering, Shenzhen University (Grant no. GDDCE 12-06). In addition, the authors would like to thank Dr. Y. W. Zhou and all study participants for their helpful discussions.

References

[1] H. Yalciner, S. Sensoy, and O. Eren, "Time-dependent seismic performance assessment of a single-degree-of-freedom frame subject to corrosion," *Engineering Failure Analysis*, vol. 19, no. 1, pp. 109–122, 2012.

[2] P. A. Sadegh, C. Dehghanian, and A. Kosari, "Corrosion protection of the reinforceing steels in chloride-laden concrete environment through exoxy/polyanilin-camphorsulfonate ," *Corrosion Science*, vol. 90, pp. 239–247, 2015.

[3] D.-E. Choe, P. Gardoni, D. Rosowsky, and T. Haukaas, "Probabilistic capacity models and seismic fragility estimates for RC columns subject to corrosion," *Reliability Engineering and System Safety*, vol. 93, no. 3, pp. 383–393, 2008.

[4] L. Berto, R. Vitaliani, A. Saetta, and P. Simioni, "Seismic assessment of existing RC structures affected by degradation phenomena," *Structural Safety*, vol. 31, no. 4, pp. 284–297, 2009.

[5] L. Berto, A. Saetta, and P. Simioni, "Structural risk assessment of corroding RC structures under seismic excitation," *Construction and Building Materials*, vol. 30, pp. 803–813, 2012.

[6] R. W. Clough, "Effect of stiffness degradation on earthquake ductility requirements," Tech. Rep. SESM66-16, Department of

Civil Engineering, University of California, Berkeley, Berkeley, Calif, USA, 1966.

[7] Z. Qu, "A collection of user-defined uniaxial hysteretic models for ABAQUS/Standard," 2007, http://www.quzhe.net/PQFiber-en.htm.

[8] S. Malekpour and F. Dashti, "Application of the direct displacement based design methodology for different types of RC structural systems," *International Journal of Concrete Structures and Materials*, vol. 7, no. 2, pp. 135–153, 2013.

[9] K. Ramin and M. Fereidoonfar, "Finite element modeling and nonlinear analysis for seismic assessment of off-diagonal steel braced RC frame," *International Journal of Concrete Structures and Materials*, vol. 9, no. 1, pp. 89–118, 2015.

[10] Y. S. Yuan, F. P. Jia, and Y. Cai, "The structural behavior deterioration model for corroded reinforced concrete beams," *China Civil Engineering Journal*, vol. 34, pp. 47–52, 2001.

[11] J.-K. Song, J. Kim, H.-B. Song, and J.-W. Song, "Effective punching shear and moment capacity of flat plate-column connection with shear reinforcements for lateral loading," *International Journal of Concrete Structures and Materials*, vol. 6, no. 1, pp. 19–29, 2012.

[12] Q.-J. Chen, J. Cai, M. A. Bradford, X. Liu, and Z.-L. Zuo, "Seismic behaviour of a through-beam connection between concrete-filled steel tubular columns and reinforced concrete beams," *Engineering Structures*, vol. 80, pp. 24–39, 2014.

[13] X. X. Chen, *Study and Evaluation on Seismic Performance of Existing Reinforced Concrete Frame*, Xi'an University of Architecture and Technology, Xi'an, China, 2011.

[14] T.-H. Kim, D.-J. Seong, and H. M. Shin, "Seismic performance assessment of hollow reinforced concrete and prestressed concrete bridge columns," *International Journal of Concrete Structures and Materials*, vol. 6, no. 3, pp. 165–176, 2012.

[15] R. He, L. H. Sneed, and A. Belarbi, "Rapid repair of severely damaged RC columns with different damage conditions: an experimental study," *International Journal of Concrete Structures and Materials*, vol. 7, no. 1, pp. 35–50, 2013.

[16] T.-H. Kim, "Comparison of totally prefabricated bridge substructure designed according to Korea Highway Bridge Design (KHBD) and AASHTO-LRFD," *International Journal of Concrete Structures and Materials*, vol. 7, no. 4, pp. 319–332, 2013.

[17] H.-S. Lee, T. Kage, T. Noguchi, and F. Tomosawa, "An experimental study on the retrofitting effects of reinforced concrete columns damaged by rebar corrosion strengthened with carbon fiber sheets," *Cement and Concrete Research*, vol. 33, no. 4, pp. 563–570, 2003.

[18] O. Ozcan, B. Binici, and G. Ozcebe, "Improving seismic performance of deficient reinforced concrete columns using carbon fiber-reinforced polymers," *Engineering Structures*, vol. 30, no. 6, pp. 1632–1646, 2008.

[19] J. Li, J. Gong, and L. Wang, "Seismic behavior of corrosion-damaged reinforced concrete columns strengthened using combined carbon fiber-reinforced polymer and steel jacket," *Construction and Building Materials*, vol. 23, no. 7, pp. 2653–2663, 2009.

[20] Y. Ma, Y. Che, and J. Gong, "Behavior of corrosion damaged circular reinforced concrete columns under cyclic loading," *Construction & Building Materials*, vol. 29, pp. 548–556, 2012.

[21] F. Biondini, E. Camnasio, and A. Titi, "Seismic resilience of concrete structures under corrosion," *Earthquake Engineering & Structural Dynamics*, vol. 44, no. 14, pp. 2445–2466, 2015.

[22] J. Lubliner, J. Oliver, S. Oller, and E. Oñate, "A plastic damage model for concrete," *International Journal of Solids and Structures*, vol. 25, no. 3, pp. 299–326, 1989.

[23] J. Lee and G. L. Fenves, "Plastic-damage model for cyclic loading of concrete structures," *Journal of Engineering Mechanics*, vol. 124, no. 8, pp. 892–900, 1998.

[24] U. Cicekli, G. Z. Voyiadjis, and R. K. Abu Al-Rub, "A plasticity and anisotropic damage model for plain concrete," *International Journal of Plasticity*, vol. 23, no. 10-11, pp. 1874–1900, 2007.

[25] S. J. George and Y. Tian, "Structural performance of reinforced concrete flat plate buildings subjected to fire," *International Journal of Concrete Structures and Materials*, vol. 6, no. 2, pp. 111–121, 2012.

[26] Y. F. Fan, Z. G. Huang, J. M. Li, and L. G. Guo, "Research on cohesive property between reinforcement and concrete of corroded RC member," *Industrial Construction*, vol. 29, pp. 49–51, 1999.

[27] H.-K. Liu and J. Li, "Constitutive law of attacked concrete," *Journal of Building Materials*, vol. 14, no. 6, pp. 736–741, 2011.

[28] GB50010, *Code for Design of Concrete Structures*, National Standard of P.R. China, Architecture &Building Press, Beijing, China, 2011.

[29] V. Birtel and P. Mark, "Parameterised finite element modelling of RC beam shear failure," in *Proceedings of the ABAQUS Users' Conference*, pp. 95–108, Boston, Mass, USA, 2006.

[30] X. L. Wang, X. Z. Lu, and L. P. Ye, "Numerical simulation for the hysteresis behavior of RC columns under cyclic loads," *Engineering Mechanics*, vol. 24, no. 12, pp. 76–81, 2007.

[31] Z. Qu, ".Predicting nonlinear response of an RC bridge pier subject to shake table motions," in *Proceedings of the 9th International Conference on Urban Earthquake Engineering (9CUEE '12)*, pp. 1717–1724, Tokyo, Japan, 2012.

[32] W.-L. Qu and Y. Wang, "Investigation on force-bearing capacity of corroded reinforced concrete beam by using nonlinear finite element analysis," *Journal of Wuhan University of Technology*, vol. 29, no. 6, pp. 73–75, 2007.

[33] W. L. Jin and J. Xia, "Influence of pitting corrosion on the bending capacity of reinforced concrete beams," *Building Structure*, vol. 39, pp. 100–102, 2009.

[34] W. P. Zhang, D. F. Shang, and X. L. Gu, "Stress-strain relationship of corroded steel bars," *Journal of Tongji University (Natural Science)*, vol. 34, no. 5, pp. 586–592, 2006.

[35] H. S. Lee, T. Noguchi, and F. Tomosawa, "FEM analysis for structure performance of deteriorated RC structures due to the corrosion of rebar," in *Proceedings of the 2nd International Conference on Concrete under Severe Conditions*, pp. 327–336, E&FN Spon, Tromso, Norway, June 1998.

[36] X. H. Wang and T. Y. Zhong, "Relation between the loss coefficient of the corroded rebar's cross-section in concrete and that of its weight," *Research and Application of Building Materials*, no. 1, pp. 4–6, 2005.

[37] MC90 CEB-FIP Model Code (1990), *Design of Concrete Structures*, British Standard Institution, London, UK, 1993.

[38] Y. Liang, X. Y. Luo, X. Q. Xiao, and Y. F. Zhang, "Experimental study on bond-slip performance of corroded reinforced concrete," *Industrial Construction*, vol. 42, no. 10, pp. 95–100, 2012.

[39] "Code for seismic design of buildings," National Standard of the People's Republic of China GB50011, China Architecture & Building Press, Beijing, China, 2010.

[40] R. Park, "Evaluation of ductility of structures and structural assemblages from laboratory testing," *Bulletin of the New*

Zealand National Society for Earthquake Engineering, vol. 22, no. 3, pp. 155–165, 1989.

[41] T. Takeda, M. A. Sozen, and N. N. Nielsen, "Reinforced concrete response to simulate earthquakes," *Journal of the Structural Division, ASCE*, vol. 96, no. 12, pp. 2557–2573, 1970.

[42] J. C. Anderson and W. H. Townsend, "Models for RC frames with degrading stiffness," *Journal of the Structural Division*, vol. 103, no. 12, pp. 2361–2376, 1977.

[43] L. F. Ibarra, R. A. Medina, and H. Krawinkler, "Hysteretic models that incorporate strength and stiffness deterioration," *Earthquake Engineering & Structural Dynamics*, vol. 34, no. 12, pp. 1489–1511, 2005.

[44] W. Shi, X. Lu, H. Guan, and L. Ye, "Development of seismic collapse capacity spectra and parametric study," *Advances in Structural Engineering*, vol. 17, no. 9, pp. 1241–1255, 2014.

[45] J. P. Ou, Z. He, B. Wu, and F. W. Qiu, "Seismic damage performance-based design of reinforced concrete structures," *Earthquake Engineering and Engineering Vibration*, vol. 19, pp. 21–30, 1999.

[46] ACI Committee 318, *Building Code Requirements for Structural Concrete and Commentary (ACI318-08)*, American Concrete Institute, Farmington Hills, Miss, USA, 2008.

[47] J. Y. Shen, *Analysis of Hysteresis Performance of the Corroded Reinforced Concrete Columns and Beams*, Zhengzhou University, Zhengzhou, China, 2014.